

# Detection, Mapping, and Proteotyping of SARS-CoV-2 Coronavirus with High Resolution Mass Spectrometry

Nicholas L. Dollman, Justin H. Griffin, and Kevin M. Downard\*

Cite This: <https://dx.doi.org/10.1021/acsinfecdis.0c00664>

Read Online

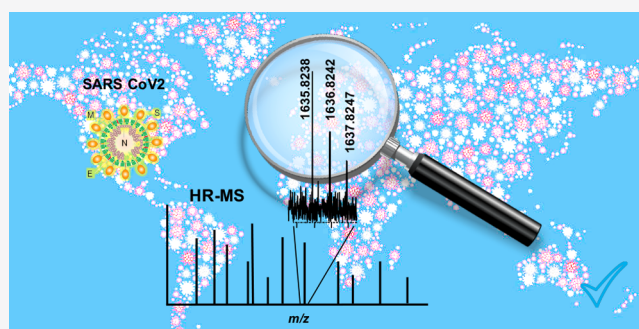
ACCESS |

Metrics &amp; More

Article Recommendations

**ABSTRACT:** A high resolution mass spectrometry approach has been applied for the first time to detect and characterize SARS-CoV-2 coronavirus in cell cultured and nasopharyngeal swab specimens. Peptide ions for three of the most abundant structural viral proteins (membrane, nucleocapsid, and spike) are detected and assigned directly, by virtue of the high resolution and mass accuracy within the mass maps of whole virus digests, without the need for tandem mass spectrometry (MS/MS). MALDI-MS based approaches offer high sample throughput and speed, compared with those of LC-MS strategies, and detection limits at some  $10^5$  copies, or orders of magnitude less with selected ion monitoring, that compete favorably with conventional reverse transcription polymerase chain reaction (RT-PCR) strategies. The detection of signature peptides unique to SARS-CoV-2 coronavirus over those from the influenza virus allows for its unambiguous detection.

**KEYWORDS:** proteotyping, SARS-CoV-2, coronavirus, virus, mass spectrometry



Since its emergence in late 2019 in Wuhan, China,<sup>1</sup> the severe acute respiratory syndrome coronavirus 2 (designated SARS-CoV-2)<sup>2</sup> has spread throughout the world and has been declared a global pandemic.<sup>3</sup> To date, it has caused over 28 million confirmed infections and close to 1 million deaths worldwide. In Australia, within a population of over 25 million, the virus is responsible for over 26 000 cases and 800 deaths, to date, as a result of border restrictions and other preventative infection control measures.<sup>3</sup> The World Health Organization has warned that the coronavirus virus is still not under control in most countries, and the cases from the pandemic continue to accelerate globally.<sup>3</sup>

The SARS-CoV-2 respiratory virus is a novel coronavirus for which there is no broad immunity, and responses have awaited the development of an effective vaccine<sup>4</sup> or other antiviral treatment.<sup>5</sup> On average, the human incubation period is 5–6 days, but it can extend to up to 14 days. The virus is transmitted from infected individuals to others who are in close contact from droplets expelled from the respiratory tract or through contact with contaminated surfaces. Common symptoms range from relatively mild illness, such as fever, a sore throat and cough, fatigue, and aches and pains, to shortness of breath and fatal pneumonia.<sup>6</sup> The virus is particularly deadly to the young and elderly.<sup>7</sup>

The virus belongs to the  $\beta$ -coronavirus family, a large class of similar viruses prevalent in a variety of hosts. Like other coronaviruses, SARS-CoV-2 consists of a single-stranded RNA genome with 29 811 nucleotide bases, about twice the size of

the influenza type A genome. It encodes four structural proteins referred to as the S (spike), E (envelope), M (membrane), and N (nucleocapsid) proteins and 24 other nonstructural and accessory proteins to facilitate replication.<sup>8</sup> The S1 subunit of the spike protein catalyzes the attachment of the virus to the membrane of a host cell, while the S2 subunit facilitates its fusion.<sup>9</sup>

Although reverse transcription polymerase chain reaction (RT-PCR) tests have been most widely employed for the detection and molecular surveillance of the virus, the current testing capacity and worldwide availability of this technology, particularly in developing countries, is struggling to meet global demand for a rapid, reliable, and widely accessible test.<sup>10</sup> Challenges remain throughout the entire analytical process, and issues with the selection and treatment of specimens, temporal variations of viral loads, and false negatives have all impacted both detection and diagnosis.<sup>11</sup>

For over two decades, this laboratory has championed, developed, and implemented novel mass spectrometry (MS) based approaches to characterize respiratory and other viruses

Received: September 21, 2020

with fine molecular detail.<sup>12,13</sup> Proteotyping approaches have been developed to identify and characterize viral proteins for surveillance,<sup>12,13</sup> type,<sup>14,15</sup> and subtype<sup>16,17</sup> strains; establish their lineage<sup>18</sup> and antigenicity;<sup>19–21</sup> and distinguish pandemic<sup>22,23</sup> and reassorted strains<sup>24</sup> from seasonal viruses.

Particular benefits of high resolution, high mass accuracy mass spectrometry have been promoted in these studies.<sup>13</sup> Viral proteins have characterized after their release and separation by gel electrophoresis<sup>25</sup> and in whole virus in clinical specimens<sup>26</sup> and virus vaccine digests.<sup>13</sup> These approaches have been particularly applied to the influenza virus, given its greatest pandemic potential, though parainfluenza viruses<sup>27</sup> and oncoviruses<sup>28</sup> in the form of hepatitis C have also been studied. High resolution MALDI based approaches are particularly suited to such surveillance strategies, due to ease of sample preparation and their high sample throughput and automation, over the application of time-consuming LC–MS/MS based<sup>29,30</sup> or low resolution MALDI-TOF approaches<sup>31</sup> recently applied to detect SARS-CoV-2.

Our proteotyping studies,<sup>12–18,22–28</sup> which largely use single signature peptides detected in mass maps to identify, type, and subtype strains should also not be confused with other uses of the term that describe, more generally, the application of protein mass spectrometry in various guises to study microorganisms. These include use of the term for what is better known as biotyping,<sup>32</sup> with and without the need for tandem mass spectrometry.

Here, for the first time, we demonstrate the power of high resolution mass spectrometry to detect and map viral proteins of the SARS-CoV-2 coronavirus. The paper represents the first to be published on the study of this virus by high resolution mass spectrometry which enables the virus to be unequivocally detected for surveillance purposes. The detection limits and a comparison with conventional RT-PCR methods are discussed.

## RESULTS

The basic protocol adopted in these experiments is shown in Figure 1. It is based on a successful method we have applied to seasonal strains of the influenza virus.<sup>26</sup> In brief, swabs used to collect SARS-CoV-2 virus specimens are washed and either grown in cell culture or prepared directly for analysis. The former produces higher virus titers and provides a more reliable approach to overcome potential false negatives associated with low viral loads in upper respiratory specimens that are known to vary greatly from infected patient to patient.<sup>33</sup>

Following filtration, the virus is precipitated and reconstituted in a digestion buffer. Any site-specific protease can be employed to digest the viral proteins, but trypsin is usually favored given its high specificity and the frequency of arginine and lysine residues. Preparation of the digests for MALDI mass analysis follows conventional protocols (see Methods section).

The incorporation of high resolution mass spectrometry into the procedure, best achieved with an FT-ICR and, to a lesser extent, an Orbitrap (Kingdon ion trap)<sup>34</sup> or extended flight TOF,<sup>35</sup> provides confidence in the peptide mass assignment so as to avoid the need for tandem mass spectrometry (MS/MS) experiments. These are both more sample-consuming (by at least an order of magnitude) and time-consuming even with modern instrumentation and automation. It also avoids the

need to interpret MS/MS spectra either manually or with computer aided software.

The high resolution MALDI mass spectrum of the whole virus digest (WVD) is shown in Figure 2. The SARS-CoV-2 virus comprises four structural proteins referred to as the S (spike), N (nucleocapsid), M (membrane), and E (envelope) proteins with molecular masses of 141.2 (for the precursor protein before cleavage into  $2 \times \sim 70$  kDa subunits), 45.6, 25.1, and 8.4 kDa, respectively. The membrane protein is the most abundant structural protein and defines the shape of the viral envelope. It and the nucleocapsid proteins are present in the highest copy numbers per virion at some 2000 and 1000 copies, respectively. The spike protein forms some 100 trimers on the surface of the virus (i.e., 300 monomers), while the envelope protein makes up only a small portion of the virion envelope comprising only some 20 copies per virion,<sup>36</sup> with most localized at the site of intracellular trafficking virus assembly and budding.

The MALDI mass spectrum is consistent with these properties, as the major ions detected correspond to segments of the nucleocapsid, membrane, and spike proteins. A total of 20 of the most abundant signals were confidently matched to segments of these three proteins with high mass accuracy (<3 ppm) (Table 1). Although present at lower copy numbers than those of the nucleocapsid and membrane proteins, the spike protein's sheer size (precursor protein mass of 141.2 kDa) ensures some of its tryptic peptides are both generated and detected in the mass map. In contrast, the envelope protein is both small (8.4 kDa) and present in low copy numbers. In addition, this protein has a dearth of trypsin cleavage residues and would generate only 4 peptides, and only two with masses less than 2500, if it were fully digested.

Within the mass range ( $m/z$  500–3000) shown (Figure 2), the peptides detected comprise 27% (8 of 30), 27% (3 of 11), and 12% (9 of 73) of all those possible for the nucleocapsid, membrane, and spike proteins. The coverage for the nucleoprotein is equivalent to that detected in a recent LC–MS based study.<sup>37</sup> In total, they are present in sufficient numbers, and appear with high mass accuracy, to allow for the unequivocal identification of the virus from the UniProt protein database.

The peptides detected also span the sequences and cover a wide range of identified N- and C-terminal, fusion peptide receptor, and RNA-binding domains (Table 1). The S1 subunit, cleaved from the precursor S spike protein at residues 685–686, mediates virus binding and entry into the host cells. The S1 subunit (residues 14–685 amino acids) contains the N-terminal domain (NTD), receptor binding domain (RBD), and receptor binding motif (RBM). The receptor binding domain (RBD) comprising residues 319–541, detected in part as peptides at  $m/z$  2039.9985 (329–346) and  $m/z$  1989.9702 (residues 387–403) (Figure 2, Table 1), binds to angiotensin-converting enzyme 2 (ACE2) receptors of susceptible host cells with high affinity. A protein comprising this domain has thus been proposed as a potential SARS-CoV-2 inhibitor.<sup>38</sup>

The remaining S2 subunit contains the fusion peptide (FP),  $\alpha$ -helical heptad repeats (HR1 and HR2), transmembrane domain (TM), and cytoplasmic domain (CP). Residues 836–847 detected at  $m/z$  1281.5859 (Figure 2, Table 1) comprise part of the fusion peptide (Figure 3). The conserved nature of this region of the protein and mechanism across the SARS-CoV, Middle East respiratory syndrome (MERS)-CoV, and SARS-CoV-2 viruses has made it an attractive target for the

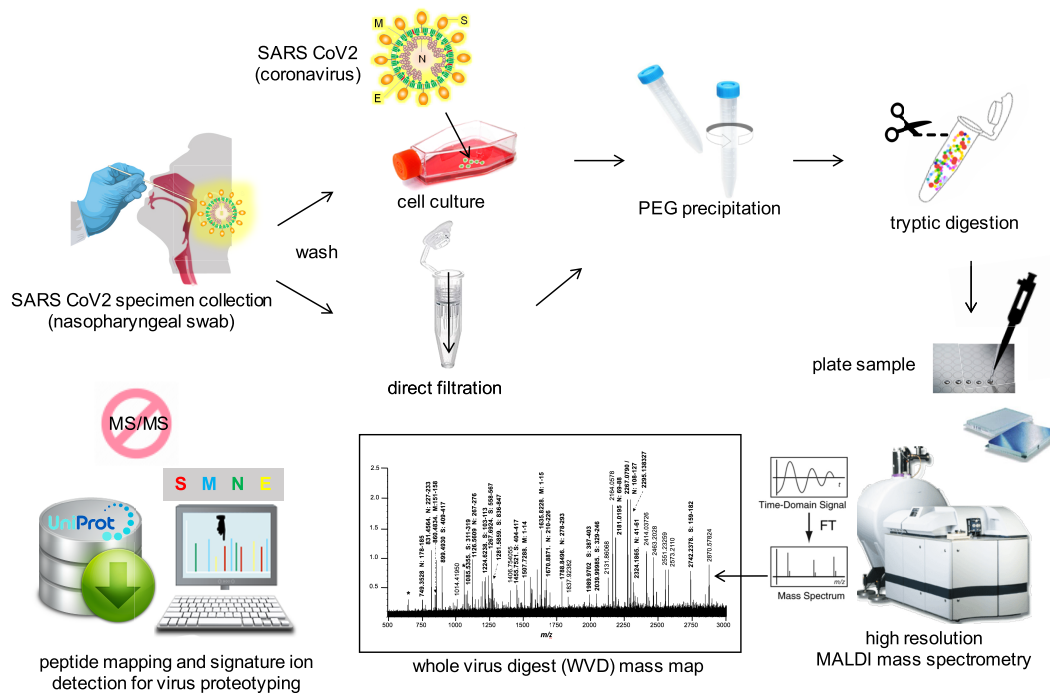


**Figure 1.** Schematic of the approach used to detect SARS-CoV-2 virus using high resolution mass spectrometry

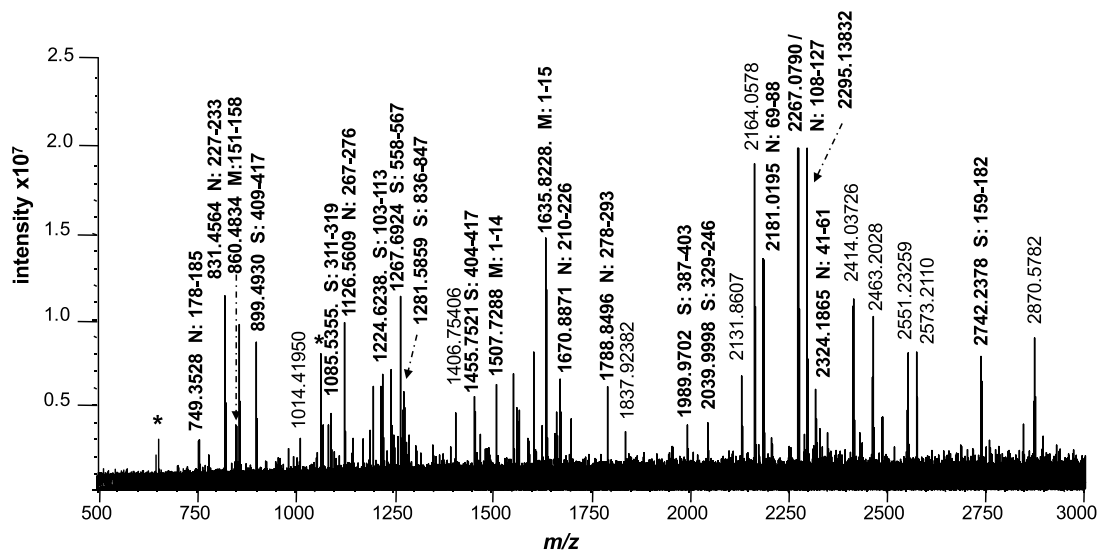


**Figure 2.** MALDI mass spectrum of the tryptic whole virus digest (WVD) peptide products of cell cultured SARS-CoV-2 virus. Peptide ions corresponding to segments of the nucleocapsid (N), membrane (M), and spike (S) proteins are shown in bold. Peaks denoted with an asterisk (\*) correspond to MALDI matrix cluster ions.

design of fusion inhibitors that can be administered against all such coronaviruses.<sup>39</sup>

Analysis of a nasopharyngeal specimen not grown in culture is shown in Figure 4. As expected, this mass spectrum shows peptide ions with reduced intensity and marked decrease in the signal-to-noise (S/N) ratio. Additional matrix cluster ions (denoted with an asterisk (\*)) are also more prominent in this spectrum. Nevertheless, despite the low virus titers, peptides for several membrane, nucleocapsid, and spike proteins are detected, including a newly detected peptide from the latter at  $m/z$  843.4255 corresponding to residues 1206–1211, beginning at the C-terminus of the HR2 domain (Figure 3) comprising residues 1162–1206. Six of these peptides were repeatedly detected in different ( $\times 10$ ) nasopharyngeal swab

specimens (Table 1), and five are reliable signature peptides ( $P_0$ ) for proteotyping<sup>13</sup> of the SARS-CoV-2 virus. They were detected in all characterized SARS-CoV-2 strains and differ in mass (by  $>3$  ppm, in greater than 95% of cases) from all influenza virus proteins of circulating strains, given the common clinical symptoms presented by this virus, using a specifically constructed algorithm and database.<sup>17</sup>

Maximum estimated levels of virus collected in nasopharyngeal swabs range from  $10^6$  to  $10^9$  copies<sup>36</sup> or up to 100-fold higher than the titers recovered from the throat (see Figure 1 of ref 36). To assess the lowest detection limits by high resolution mass spectrometry, the most abundant peptide signal at  $m/z$  1635.8238 (membrane protein residues M = 1–15) (see inset showing resolved isotopic cluster in Figure 4 and

**Table 1.** Tryptic Peptide Ions of Structural Viral Proteins Detected in WVD Spectrum, Their Sequences, Detection in Nasal Swabs, Use as a Signature, and Location

<i>m/z</i> (mono) experimental	<i>m/z</i> (mono) theoretical	differential (diff, ppm)	viral protein code	residues <sup>a</sup>	sequence	replicate in nasal washes (×10)	signature ( <i>P</i> <sub>o</sub> > 0.95)	domain <sup>b</sup>
749.3528	749.3536	-1.0	N	178–185	GGSQASSR			RNA-binding domain
831.4564	831.4570	-0.7	N	227–233	LNQLESK			dimerization domain
843.4255	843.4247	+0.9	S	1206–1211	YEQYIK	✓	✓	includes HR2 domain
860.4834	860.4849	-1.7	M	151–158	IAGHHLGR	✓	X	undefined
899.4930	899.4945	-1.6	S	409–417	QIAPGQTGK			S1 subunit C-terminal domain (CTD)
1085.5355	1085.5374	-1.7	S	311–319	GIYQTSNFR			undefined
1126.5609	1126.5640	-2.7	N	267–276	AYNVTVQAFGR	X	✓	dimerization domain
1224.6238	1224.6259	-1.7	S	103–113	GWIFGTTLDSK			S1 subunit N-terminal domain (NTD)
1267.6924	1267.6946	-1.7	S	558–567 (1)	KFLPFQQFGR			undefined
1281.5859	1281.5892	-2.5	S	836–847	QYGDCLGDIAAR			S2 subunit fusion peptide (FP)
1455.7521	1455.7550	-1.9	S	404–417 (1)	GDEVQRQIAPGQTGK			S1 subunit C-terminal domain (CTD)
1507.7288	1507.7308	-1.3	M	1–14	MADSNGTITVEELK			virion surface region
1635.8228	1635.8258	-1.8	M	1–15(1)	MADSNGTITVEELKK	✓	✓	virion surface region
1670.8871	1670.8894	-1.3	N	210–226	MAGNGGDAALALLLLDR	✓	✓	undefined
1788.8498	1788.8511	-0.7	N	278–293	GPEQTQGNFNGDQELIR			dimerization domain
1989.9702	1989.9738	-1.8	S	387–403	LNDLCFTNVYADSFVIR	✓	✓	S1 subunit receptor binding domain (RBD)
2039.9985	2040.0007	-1.0	S	329–346	FPNITNLCPFGEVFNATR			S1 subunit receptor binding domain (RBD)
2181.0195	2181.0207	-0.5	N	69–88	GQGVPIINTSSPDDQIGYYR			RNA-binding domain
2267.0790	2267.0807	-0.7	N	108–127	WYFYFLGTGPEAGLPYGANK	✓	X	N-terminal domain (NTD)
2324.1865	2324.1894	-1.2	N	41–61 (1)	RPQGLPNNTASWFTALTQHGK			RNA-binding domain
2742.2378	2742.2425	-1.7	S	159–182	VYSSANNCTFEYVSQPFMLDLEGK			S1 subunit N-terminal domain (NTD)

<sup>a</sup>Residues denoted with a (1) are associated with one missed cleavage site; all others contain no missed cleavage sites. <sup>b</sup>As defined on UniProt knowledge base (uniprotkb) at <https://covid-19.uniprot.org/uniprotkb/>.

sequence in bold in Table 1) was monitored following serial dilution of the cell cultured sample. The results are shown in Figure 5.

The virus is detected based on this peptide down to 0.75 ng with a signal-to-noise ratio of 3:1. Given that the virus particle has been estimated to have a total mass of 1 fg,<sup>36</sup> this corresponds to  $7.5 \times 10^5$  copies. The actual amount of virus consumed to generate the spectra is less than this value, because only a relatively small portion of the sample is ablated, ionized, and detected in MALDI mass spectrometry. Furthermore, the use of selected ion monitoring of one or several of the predicted peptides over acquisition of a full range mass spectrum would appreciably lower this value.

The copy number, nevertheless, compares favorably with the  $10^5$ – $10^6$  copies of virus required for high quality PCR sequencing but is currently higher than the  $10^3$ – $10^4$  copies typically required for detection. It is consistent with an earlier study we have reported for the influenza virus.<sup>26</sup> With single ion detection of the signature ions, it is also compatible currently to the  $10^3$ – $10^4$  copies typically required for PCR detection.

## DISCUSSION

Despite the widespread use of RT-PCR methods to detect and characterize SARS-CoV-2 viruses during the pandemic, the steps involved are not insignificant.<sup>41</sup> RNA extraction is followed by reverse transcription and the amplification of

cDNA using a pair of upstream and downstream primers following purification using magnetic beads. The products are either detected using hybridization assays, typically targeting conserved regions of the nucleocapsid gene or those of the envelope (E), spike (S), or a polymerase protein, or employing chain termination chemistries where sequencing is required. Total analysis times take at least 24–48 h.

Furthermore, despite a general high degree of genetic conservation, some evolution of the virus has been detected so that the binding sites of primers and probes should be continuously monitored.<sup>11</sup> High rates of false-negative SARS-CoV-2 RT-PCR results and prolonged nucleic acid conversion have been reported in some studies.<sup>11</sup> The cost of an RT-PCR instrument ranges from some \$AUD 20 000 to over \$AUD 100 000 with sequencing costs ranging from \$AUD 1 to 10 per megabase (Mb).

In contrast, the MS approach described here requires no separation of viral components. The pretreatment of samples (chemical modification and proteolysis) can be expedited and performed in a similar time frame to those steps necessary for PCR based methods. The design of the MALDI target plate makes it possible for mass spectra to be acquired from hundreds of digested virus samples within a few minutes, while the time for virus pretreatment and proteolytic digestion can be minimized by using immobilized enzymes at higher enzyme to protein ratios and by processing many samples in parallel. Coupled to automated, or semiautomated, spectral acquisition,

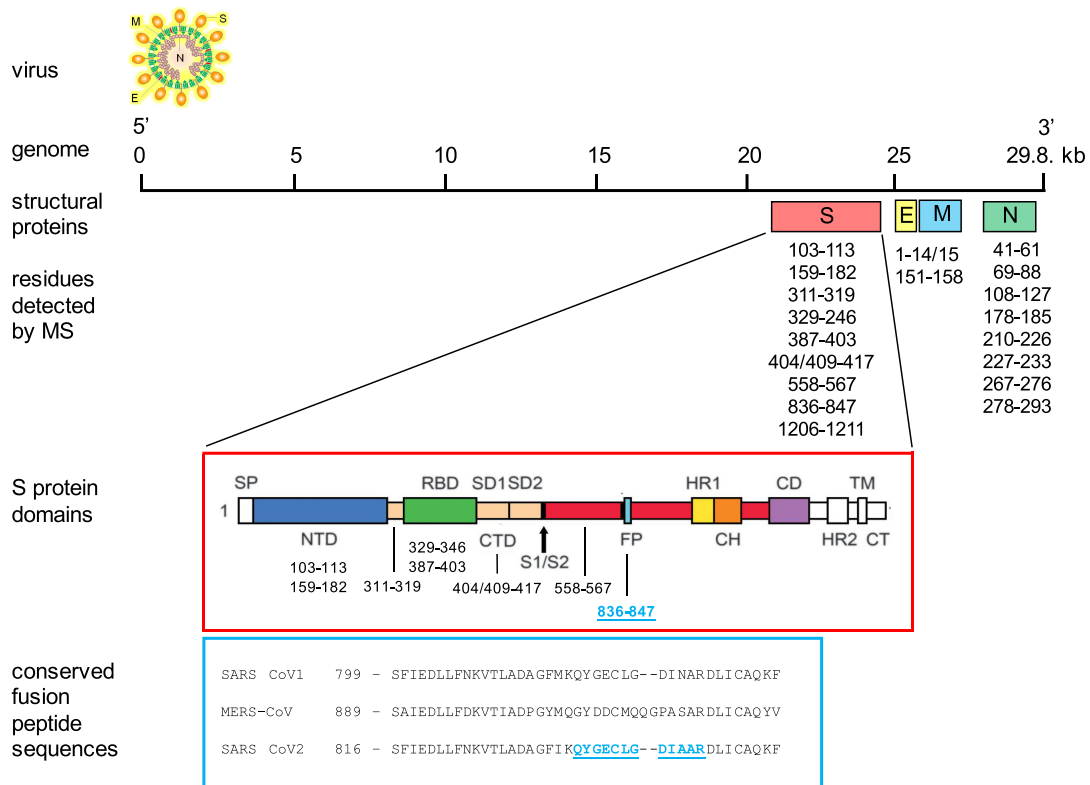


**Figure 3.** Coding region of the SARS-CoV-2 genome for the spike (S), envelope (E), membrane (M) and nucleocapsid (N) proteins showing the peptide segments detected for each protein and their position within the domains of the former.

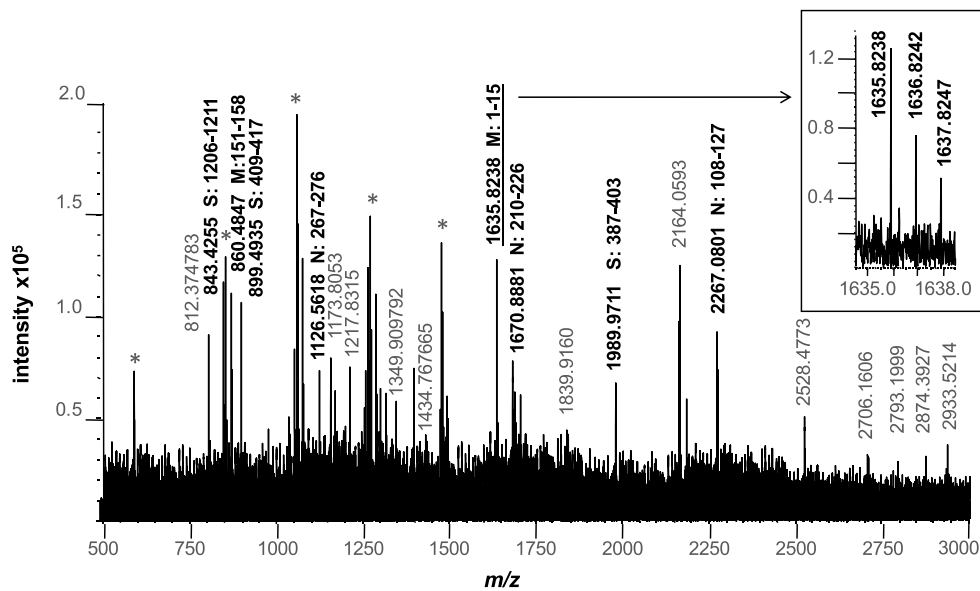


**Figure 4.** MALDI mass spectrum of the tryptic digest products of nasopharyngeal swab recovered whole virus SARS-CoV-2 virus. Peaks denoted with an asterisk (\*) correspond to MALDI matrix cluster ions.

hundreds of samples can be analyzed in a relatively short period of time.

MALDI mass spectrometry is inherently faster than LC-MS based strategies<sup>29,30</sup> where the, often overlooked and under reported, time to set up HPLC conditions and equilibrate and flush columns between runs adds to the analysis time and must be considered. The use of reverse phase columns is also accompanied by some unavoidable sample loss which reduces the sensitivity of such an approach. MALDI based instruments

are more amenable to in-field applications, and small and portable mass spectrometers are being developed<sup>42</sup> with ever improving performance. Although a high resolution mass spectrometer, required to confidently assign viral peptides from mass map data without any MS/MS sequencing, has a considerable cost (some \$AUD 500 000 to 1 000 000), it is a one-time cost and not inconsistent with the costs required for multiple PCR sequencers and associated equipment.

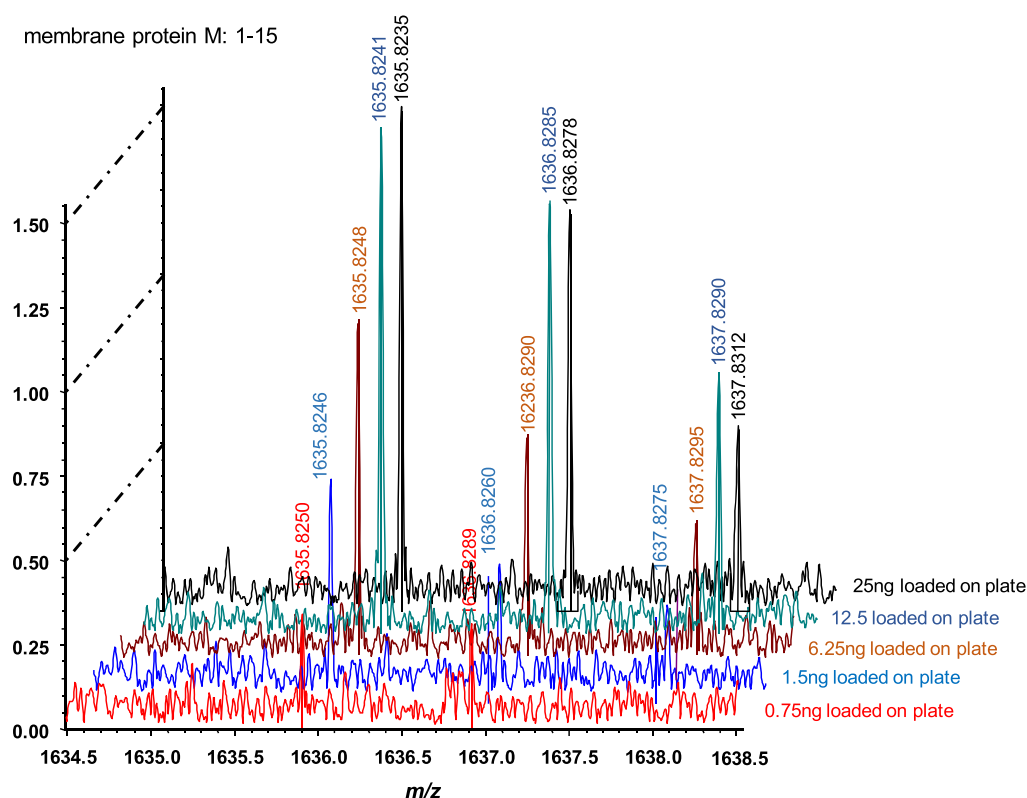


**Figure 5.** MALDI mass spectrum of peptide ions at  $m/z$  1635.8 from the membrane protein (residues 1–15) as a function of virus loaded onto the sample plate according to real time PCR.<sup>40</sup>

Detection limits, which have been demonstrated here and in our earlier study<sup>26</sup> to be of the order of  $10^5$  copies, could be substantially improved by adopting automated single ion monitoring (SIM) strategies that seek to detect only selected signature peptides for proteotyping rather than record full mass range spectra. The sensitivity is increased by a factor equivalent to that of the reduction in the scan time; that is, by reducing the scan time by a factor of 10, a 10-fold increase in sensitivity would be attained.

## CONCLUSIONS

The rapid global spread of the SARS-CoV-2 virus and its mounting health and economic costs requires the development and application of all possible diagnostic approaches in our scientific arsenal to mitigate its effects. This study demonstrates the power of high resolution, high mass accuracy mass spectrometry to detect and characterize the SARS-CoV-2 virus. It adds to a series of studies reported from this laboratory employing high resolution mass spectrometry to type, subtype, and establish the lineage and study the evolution of respiratory viruses such as influenza and parainfluenza reported by this laboratory.<sup>12–27</sup> Mass spectrometry with proteotyping using signature peptides,<sup>13</sup> given its sensitivity, speed, and high throughput, should play a greater role in the frontline molecular detection of SARS-CoV-2, other respiratory viruses, and biopathogens in the near future and represents an important and viable complement to PCR based and other biochemical detection methods.<sup>43</sup> It complements mass spectrometric methods for quantify glycosylation levels across strains to aid future vaccine production.<sup>44</sup>

## METHODS

**Specimen Preparation.** All procedures for collection, preparation, and transport of the samples were carried out in accordance with the Communicable Diseases Network Australia (CDNA) national guidelines for Coronavirus Disease 2019 and NSW Health restrictions and protocols. SARS-CoV-2 specimens were collected from infected patients using nasopharyngeal swabs. These are inserted approximately 2–3 cm into the nostril, to the anterior end of the nasal turbinate, parallel to the palate (Figure 1). Upon collection, specimens were placed in a saline solution and stored at  $-70$  °C.

Specimens confirmed to contain SARS-CoV-2 were grown in cell culture or analyzed directly. The virus was cultured in Vero E6 cells<sup>45</sup> in (Dulbecco's Modified Eagle Medium) (Sigma-Aldrich) supplemented with 10% heat-inactivated fetal bovine serum (FBS) following a reported procedure<sup>33</sup> within a physical containment laboratory. Cells were completely inactivated; first, they were inactivated chemically with formalin (1%) buffered solution at room temperature, and then, they were heat inactivated at 100 °C for 15 min<sup>45</sup> and stored at  $-70$  °C before further use. Polyethylene glycol precipitation of the virus was performed after filtration in a manner similar to that reported.<sup>26</sup> Nasopharyngeal swabs used directly were washed with saline ( $3 \times 3$  mL) and purified water ( $2 \times 1.5$  mL) and then passed through a 300 K molecular weight cutoff (MWCO) filter (Pall Corporation, Cheltenham, Victoria) prior to collection and concentration of the retentate for digestion and analysis.

**In-Solution Whole Virus Tryptic Digests.** Virus pellets were reconstituted in 100  $\mu$ L of digestion buffer (50 mM ammonium bicarbonate, 10% acetonitrile, 2 mM dithiothreitol, and 5 mM octyl  $\beta$ -D-glucopyranoside) at pH 7.5, sonicated for

20 min, incubated for 2 h at 37 °C, and digested overnight following the addition of 15 ng/ $\mu$ L sequencing-grade modified trypsin (Promega Corporation, Sydney, Australia).

**High Resolution MALDI-FT-ICR Mass Spectrometry.** Solutions of viral peptides (1  $\mu$ L) were diluted with a solution (5  $\mu$ L) of matrix (5 mg/mL  $\alpha$ -cyano-4-hydroxycinnamic acid in 50% acetonitrile with 0.1% trifluoroacetic acid). Solution volumes of 1  $\mu$ L were spotted onto a matrix-assisted laser desorption ionization Fourier-transform ion cyclotron resonance (MALDI-FT-ICR) mass spectrometry sample plate and analyzed as previously described.<sup>29</sup> The instrument was calibrated externally with a standard peptide mixture, and tryptic peptides were identified based on the reported sequences of the SARS-CoV-2 viral proteins.

**Protein Sequences of SARS-CoV-2 Virus.** Protein sequences for the four structural proteins of the SARS-CoV-2 virus were downloaded from the Uniprot protein database (<https://covid-19.uniprot.org/>). These were digested *in silico* using the ExPASy PeptideMass tool ([https://web.expasy.org/peptide\\_mass/](https://web.expasy.org/peptide_mass/)).

## AUTHOR INFORMATION

### Corresponding Author

Kevin M. Downard – Infectious Disease Responses  
Laboratory, Prince of Wales Clinical Sciences Research,  
Sydney, NSW 2031, Australia;  [orcid.org/0000-0003-0904-4141](https://orcid.org/0000-0003-0904-4141); Phone: +61 2 9382 2886;  
Email: [kevin.downard@scientia.org.au](mailto:kevin.downard@scientia.org.au)

### Authors

Nicholas L. Dollman – Infectious Disease Responses  
Laboratory, Prince of Wales Clinical Sciences Research,  
Sydney, NSW 2031, Australia  
Justin H. Griffin – Infectious Disease Responses Laboratory,  
Prince of Wales Clinical Sciences Research, Sydney, NSW  
2031, Australia

Complete contact information is available at:  
<https://pubs.acs.org/10.1021/acscinfecdis.0c00664>

### Notes

The authors declare no competing financial interest.

## ACKNOWLEDGMENTS

K.M.D. thanks staff at the Prince of Wales Hospital for information and advice and donors who have supported this study. The mass spectrometer was purchased with funds from the Australian Research Council.

## REFERENCES

- (1) Li, Q., Guan, X., Wu, P., Wang, X., Zhou, L., Tong, Y., Ren, R., Leung, K. S. M., Lau, E. H. Y., Wong, J. Y., Xing, X., Xiang, N., Wu, Y., Li, C., Chen, Q., Li, D., Liu, T., Zhao, J., Liu, M., Tu, W., Chen, C., Jin, L., Yang, R., Wang, Q., Zhou, S., Wang, R., Liu, H., Luo, Y., Liu, Y., Shao, G., Li, H., Tao, Z., Yang, Y., Deng, Z., Liu, B., Ma, Z., Zhang, Y., Shi, G., Lam, T. T. Y., Wu, J. T., Gao, G. F., Cowling, B. J., Yang, B., Leung, G. M., and Feng, Z. (2020) Early transmission dynamics in Wuhan, China, of novel coronavirus-infected pneumonia. *N. Engl. J. Med.* 382, 1199–1207.
- (2) Chauhan, S. (2020) Comprehensive review of coronavirus disease 2019 (COVID-19). *Biomedical J.* 43, 334–340.
- (3) World Health Organisation, Covid 2019, <https://covid19.who.int> (accessed 2020-07-14).
- (4) Logunov, D. Y., Dolzhikova, I. V., Zubkova, O. V., Tukhvatullin, A. I., Shcheblyakov, D. V., Dzhavakava, A. S., Grousova, D. M.,

Erokhova, A. S., Kovyryshina, A. V., Botikov, A. G., Izhaeva, F. M., Popova, O., Ozharovskaya, T. A., Esmagambetov, I. B., Favorskaya, I. A., Zrelkin, D. I., Voronina, D. V., Shcherbinin, D. N., Semikhin, A. S., Simakova, Y. V., Tokarskaya, E. A., Lubenets, N. L., Egorova, D. A., Shmarov, M. M., Nikitenko, N. A., Morozova, L. F., Smolyarchuk, E. A., Kryukov, E. V., Babira, V. F., Borisevich, S. V., Naroditsky, B. S., and Gintsburg, A. L. (2020) Safety and immunogenicity of an rAd26 and rAd5 vector-based heterologous prime-boost COVID-19 vaccine in two formulations: two open, non-randomised phase 1/2 studies from Russia. *Lancet* 396, P887–897.

(5) Jean, S. S., Lee, P. I., and Hsueh, P. R. (2020) Treatment options for COVID-19: The reality and challenges. *J. Microbiol. Immunol. Infect.* 5, 436–443.

(6) Wang, L., Wang, Y., Ye, D., and Liu, Q. (2020) Review of the 2019 novel coronavirus (SARS-CoV-2) based on current evidence. *Int. J. Antimicrob. Agents* 55, 105948.

(7) Davies, N. G., Klepac, P., Liu, Y., et al. (2020) Age-dependent effects in the transmission and control of COVID-19 epidemics. *Nat. Med.* 26, 1205–1211.

(8) Astuti, I., and Ysrafil, Y. (2020) Severe Acute Respiratory Syndrome Coronavirus 2 (SARS-CoV-2): An overview of viral structure and host response. *Diabetes Metab. Syndr.* 14, 407–412.

(9) Li, F. (2016) Structure, Function, and Evolution of Coronavirus Spike. *Annu. Rev. Virol.* 3, 237–261.

(10) Feng, W., Newbigging, A. M., Le, C., Pang, B., Peng, H., Cao, Y., Wu, J., Abbas, G., Song, J., Wang, D.-B., Cui, M., Tao, J., Tyrrell, D. L., Zhang, X.-E., Zhang, H., and Le, X. E. (2020) Molecular Diagnosis of COVID-19: Challenges and Research Needs. *Anal. Chem.* 92, 10196–10209.

(11) Woloshin, S., Patel, N., and Kesselheim, A. S. (2020) False Negative Tests for SARS-CoV-2 Infection - Challenges and Implications. *N. Engl. J. Med.* 383, e38.

(12) Downard, K. M., and Morrissey, B. (2007) Fingerprinting a Killer - Surveillance of the Influenza Virus by Mass Spectrometry. *Analyst* 132, 611–614.

(13) Downard, K. M. (2013) Proteotyping for the Rapid Identification of Pandemic Influenza Virus and other Biopathogens. *Chem. Soc. Rev.* 42, 8584–8595.

(14) Schwahn, A. B., Wong, J. W. H., and Downard, K. M. (2009) Signature peptides of influenza nucleoprotein for the typing and subtyping of the virus by high resolution mass spectrometry. *Analyst* 134, 2253–2261.

(15) Schwahn, A. B., Wong, J. W. H., and Downard, K. M. (2010) Typing of Human and Animal Strains of Influenza Virus with Conserved Signature Peptides of Matrix M1 Protein by High Resolution Mass Spectrometry. *J. Virol. Methods* 165, 178–185.

(16) Nguyen, A. P., and Downard, K. M. (2013) Subtyping of Influenza Neuraminidase using Mass Spectrometry. *Analyst* 138, 1787–1793.

(17) Schwahn, A. B., Wong, J. W. H., and Downard, K. M. (2010) Rapid typing and subtyping of vaccine strains of the influenza virus with high resolution mass spectrometry. *Eur. J. Mass Spectrom.* 16, 321–329.

(18) Schwahn, A. B., and Downard, K. M. (2011) Proteotyping to establish the lineage of type A H1N1 and type B human influenza virus. *J. Virol. Methods* 171, 117–122.

(19) Kiselar, J. G., and Downard, K. M. (1999) Antigenic Surveillance of the Influenza Virus by Mass Spectrometry. *Biochemistry* 43, 14185–14191.

(20) Morrissey, B., Streamer, M., and Downard, K. M. (2007) Antigenic Characterisation of H3N2 subtypes of the Influenza Virus by Mass Spectrometry. *J. Virol. Methods* 145, 106–114.

(21) Schwahn, A. B., and Downard, K. M. (2009) Antigenicity of a type A influenza virus through a comparison of hemagglutination inhibition and mass spectrometry immunoassays. *J. Immunoassay Immunochem.* 30, 245–261.

(22) Schwahn, A. B., Wong, J. W. H., and Downard, K. M. (2010) Rapid Differentiation of Seasonal and Pandemic H1N1 Influenza

through Proteotyping of Viral Neuraminidase with Mass Spectrometry. *Anal. Chem.* 82, 4584–4590.

(23) Fernandes, N. D., and Downard, K. M. (2014) Origins of the Reassortant H1N1 2009 Pandemic Influenza Virus by Proteotyping with Mass Spectrometry. *J. Mass Spectrom.* 49, 93–102.

(24) Lun, A. T. L., Wong, J. W. H., and Downard, K. M. (2012) FluShuffle and FluResort - New Algorithms to Identify Reassorted Strains of the Influenza Virus by Mass Spectrometry. *BMC Bioinf.* 13, 208.

(25) Morrissey, B., and Downard, K. M. (2006) A Proteomics Approach to Survey the Antigenicity of the Influenza Virus by Mass Spectrometry. *Proteomics* 6, 2034–2041.

(26) Fernandes, N. D., and Downard, K. M. (2014) Incorporation of a Proteotyping Approach using Mass Spectrometry for the Surveillance of the Influenza Virus in Cell Culture. *J. Clin. Microbiol.* 52, 725–735.

(27) Nguyen, A. P., and Downard, K. M. (2013) Proteotyping of the Parainfluenza Virus with High Resolution Mass Spectrometry. *Anal. Chem.* 85, 1097–1105.

(28) Uddin, R., and Downard, K. M. (2017) Subtyping of Hepatitis C Virus with High Resolution Mass Spectrometry. *Clin. Mass Spectrom.* 4–5, 19–24.

(29) Singh, P., Chakraborty, R., Marwal, R., Radhakrishnan, V. S., Bhaskar, A. K., Vashisht, H., Dhar, M. S., Pradhan, S., Ranjan, G., Imran, M., Raj, A., Sharma, U., Singh, P., Lall, H., Dutta, M., Garg, P., Ray, A., Dash, D., Sivasubbu, S., Gogia, H., Madan, P., Kabra, S., Singh, S. K., Agrawal, A., Rakshit, P., Kumar, P., and Sengupta, S. (2020) A rapid and sensitive method to detect SARS-CoV-2 virus using targeted-mass spectrometry. *J. Proteins Proteomics* 11, 159–165.

(30) Gouveia, D., Grenga, L., Gaillard, J.-C., Gallais, F., Bellanger, L., Pible, O., and Armengaud, J. (2020) Shortlisting SARS-CoV-2 Peptides for Targeted Studies from Experimental Data-Dependent Acquisition Tandem Mass Spectrometry Data. *Proteomics* 20, e2000107.

(31) Nachtigall, F. M., Pereira, A., Trofymchuk, O. S., and Santos, L. B. (2020) Detection of SARS-CoV-2 in nasal swabs using MALDI-MS. *Nat. Biotechnol.* 38, 1168–1173.

(32) Karlsson, R., Gonzales-Siles, L., Boulund, F., et al. (2015) Proteotyping: Proteomic characterization, classification and identification of microorganisms - A prospectus. *Syst. Appl. Microbiol.* 38, 246–257.

(33) Zou, L., Ruan, F., Huang, M., et al. (2020) SARS-CoV-2 Viral Load in Upper Respiratory Specimens of Infected Patients. *N. Engl. J. Med.* 382, 1177–1179.

(34) Eliuk, S., and Makarov, A. (2015) Evolution of Orbitrap Mass Spectrometry Instrumentation. *Annu. Rev. Anal. Chem.* 8, 61–80.

(35) Satoh, T., Sato, T., and Tamura, J. (2007) Development of a high-performance MALDI-TOF mass spectrometer utilizing a spiral ion trajectory. *J. Am. Soc. Mass Spectrom.* 18, 1318–1323.

(36) Bar-On, Y. M., Flamholz, A., Phillips, R., and Milo, R. (2020) SARS-CoV-2 (COVID-19) by the numbers. *eLife* 9, e57309.

(37) Nikolaev, E. N., Indeykina, M. I., Brzhozovskiy, A. G., Bugrova, A. E., Kononikhin, A. S., Starodubtseva, N. L., Petrotchenko, E. V., Kovalev, G. I., Borchers, C. H., and Sukhikh, G. T. (2020) Mass-Spectrometric Detection of SARS-CoV-2 Virus in Scrapings of the Epithelium of the Nasopharynx of Infected Patients via Nucleocapsid N Protein. *J. Proteome Res.*, DOI: 10.1021/acs.jproteome.0c00412.

(38) Tang, T., Bidon, M., Jaimes, J. A., Whittaker, G. R., and Daniel, S. (2020) Coronavirus membrane fusion mechanism offers a potential target for antiviral development. *Antiviral Res.* 178, 104792.

(39) Tai, W., He, L., Zhang, X., Pu, J., Voronin, D., Jiang, S., Zhou, Y., and Du, L. (2020) Characterization of the receptor-binding domain (RBD) of 2019 novel coronavirus: implication for development of RBD protein as a viral attachment inhibitor and vaccine. *Cell. Mol. Immunol.* 17, 613–620.

(40) Keyaerts, E., Vijgen, L., Maes, P., Dusion, G., Neyts, J., and Ransta, M. V. (2006) Viral load quantitation of SARS-coronavirus RNA using a one-step real-time RT-PCR. *Int. J. Infect. Dis.* 10, 32–37.

(41) da Silva, S. J. R., da Silva, C. T. A., Guarines, K. M., Mendes, R. P. G., Pardee, K., Kohl, A., and Pena, L. (2020) Clinical and Laboratory Diagnosis of SARS-CoV-2, the Virus Causing COVID-19. *ACS Infect. Dis.* 6, 2319–2336.

(42) Ding, L., Sudakov, M., Brancia, F. L., Giles, R., and Kumashiro, S. (2004) A digital ion trap mass spectrometer coupled with atmospheric pressure ion sources. *J. Mass Spectrom.* 39, 471–484.

(43) McEwen, C. M., Ligler, F. S., and Swager, T. M. (2013) Chemical and biological detection. *Chem. Soc. Rev.* 42, 8581–8583.

(44) Sun, Z., Ren, K., Zhang, X., Chen, J., Jiang, Z., Jiang, J., Ji, F., Ouyang, X., and Li, L. (2020) Mass Spectrometry Analysis of Newly Emerging Coronavirus HCoV-19 Spike Protein and Human ACE2 Reveals Camouflaging Glycans and Unique Post-Translational Modifications. *Engineering*, in press.

(45) Jureka, A. S., Silvas, J. A., and Basler, C. F. (2020) Propagation, Inactivation, and Safety Testing of SARS-CoV-2. *Viruses* 12, 622.